Characterization of Immune Infiltrate and Checkpoint Protein Expression Patterns in Murine Syngeneic Tumors via Multiplex Immunohistochemistry

Jennifer Ziello, Sarah Klein, Katrina Costa, Katherine Crosby
Cell Signaling Technology, Inc., Danvers MA 01923

Abstract # 5689

INTRODUCTION

Murine syngeneic tumor models are increasingly utilized for preclinical immuno-oncology studies as immunotherapeutic strategies continue to make clinical strides. However, the immunologic features of the tumor microenvironment (TME) in these models remain largely undefined. In this study, we applied a 7-color multiplex immunohistochemistry (mIHC) panel to visualize and quantify the immune infiltrate within formalin-fixed, paraffin-embedded (FFPE) Renca, CT26, and LL/2 tumor tissues derived from subcutaneous mouse models of renal cell carcinoma, colon carcinoma, and lung carcinoma, respectively. Additionally, we applied this panel to a 4T1 orthotopic primary mammary tumor and 4T1 lung metastasis formed via tail vein injection. The multiplex panel included antibodies detecting CD3 and CD8 as T cell markers, F4/80 as a myeloid cell marker, the immunosuppressive receptor PD-1, as well as its ligand PD-L1, pan-keratin as a tumor mask, and DAPI as a nuclear counterstain. We characterized the localization of tumor-infiltrating immune cells, as well as trends in the coexpression and frequency patterns of immunosuppressive proteins. This study strives to better understand the underlying differences in the immunologic landscapes of these tumors, which in turn has implications for researchers studying responses to immunotherapeutic approaches and combination strategies in murine models of cancer.

METHODS

A mIHC panel was optimized and applied to 5 FFPE murine syngeneic tumor sections as well as to 1 normal murine lung section. Tumors derived from Renca, LL/2, and CT26 cell lines, as well as a 4T1-derived orthotopic mammary tumor and lung metastasis were stained with the 7-plex panel below (Table 1), spectrally unmixed with a Mantra™ Quantitative Pathology Workstation (PerkinElmer), and quantitatively analyzed using the inForm® Tissue Finder™ software (PerkinElmer). Three fields per tissue were imaged and used for quantification. This quantification included analysis of parameters such as total cell counts positive for each phenotypic marker and colocalization or coregistration of signal. This protocol allows for the simultaneous use of multiple rabbit monoclonal antibodies. In order to avoid mouse-on-mouse reactivity, all antibodies included in this panel were raised in rabbit, with the exception of pan keratin, which was a biotinylated mouse antibody that was detected via HRP-streptavidin followed by an AF350 tyramide conjugate. The following antibodies from Cell Signaling Technology, Inc. were used with the conditions listed in Table 1A for the staining of this panel.

CHALLENGES

- The irregular shape and projections of F4/80+ cells made them exceptionally difficult to segment and analyze accurately. Rather than providing a measurement of the frequency of coexpression of various targets with F4/80, the presented numbers are more reflective of coregistration, where a given target is either coexpressed with F4/80, in close proximity to a cell expressing F4/80, or expressed on a cell being engulfed or encircled by an F4/80+ cell.
- A subset of CD3-/CD8+ cells was observed. A fraction of these cells stained positively for CD11c , indicating that they are dendritic cells. Alternatively, this subset could be natural killer cells. Feng, et al. have observed similar subsets of CD3-/CD8+ cells in similar multiplex panels applied to normal mouse spleen (Feng, et al.; 2016).

CONCLUSIONS

- The LL/2 and Renca tumors were the least infiltrated with respect to T cells.
- PD-1+ T cells were observed in all tumors, yet not in the normal lung tissue that was tested.
- In general, PD-1 was not found on CD8+ T cells but rather localized to other cell types in the tumors tested.
- PD-L1 expression was observed on macrophages in all tumors tested.
- Striking differences were observed in the profiles of the 4T1 mammary tumor vs the 4T1 lung metastasis (see Figure 4A):
- Coregistration of PD-L1 with F4/80 occurred more frequently in the 4T1 lung metastasis than the 4T1 primary tumor.
- The 4T1 lung metastasis harbored the highest numbers of F4/80+ infiltrate, while the 4T1 mammary primary tumor harbored the fewest number of F4/80+ infiltrate of the tumor samples.
- The 4T1 mammary tumor contained the most PD-L1+ cells. Of those PD-L1+ cells, however, a much lower percentage coregistered with F4/80 than in any of the other syngeneic tumors.
- Overall, this study highlights the diverse immune landscape among murine syngeneic tumor models as well as between primary and metastatic sites with respect to unique cell subsets and PD-1/PD-L1 expression patterns. A set of robustly validated IHC antibodies, along with in-depth optimization to develop the precise conditions of the multiplex panel, is required for the accurate identification and deconvolution of these subsets.

REFERENCES

Feng Z, et al. *J Immunol.*
Oft M, et al. *Current Biol.* 1998;8:1243-1252.

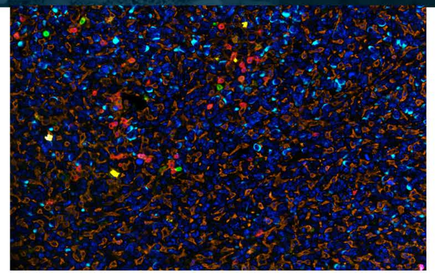

LL/2 tumor tissue stained with the described panel (Table 1).

Table 1A

Antibody	Product #	Dilution	Fluorophore Pairing	Order
CD3e (D4V8L)	99940	1:300	Cy5	1st
PD-1 (D7D5W)	84651	1:100	FITC	2nd
CD8 (D4W2Z)	98941	1:300	AF594	3rd
PD-L1 (D5V3B)	64988	1:50	AF555	4th
F4/80 (D2S9R)	70076	1:500	Cy5.5	5th
Pan keratin (C11)	4279	1:50	AF350	6th

Figure 1A

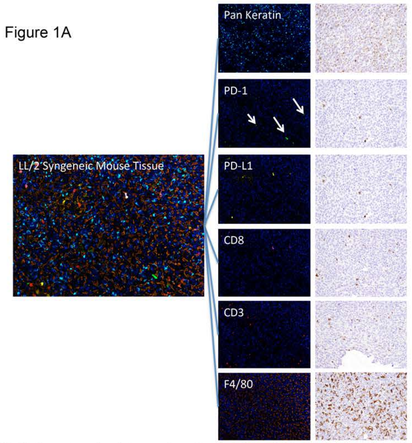

Table 1A. The optimized conditions used to stain each tissue section.
Figure 1A. A syngeneic mouse LL/2 tumor was stained with the 7-plex mIHC panel previously described. The composite image is shown on the left with the fluorescent breakdown on the right, adjacent to chromogenic staining performed on serial sections.

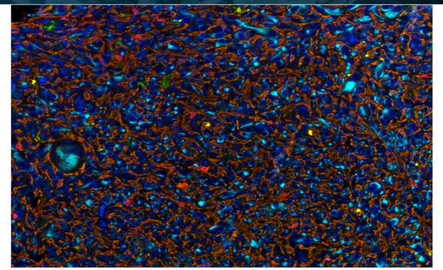

Renca tumor tissue stained with the described panel (Table 1).

Figure 2A

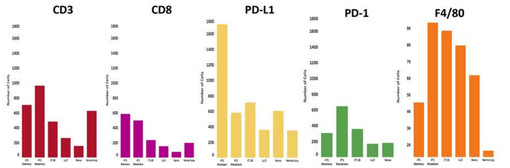

Figure 2B

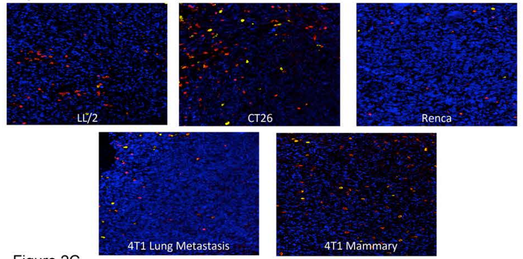

Figure 2C

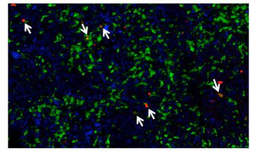

Figure 2A. Total cell counts positive for each target stained across all 3 fields imaged of each syngeneic tumor, as well as the normal lung tissue.
Figure 2B. Representative images of CD3+ and CD8+ cells present in Renca, CT26, LL/2, 4T1 lung metastasis and 4T1 mammary tumors (from left to right).
Figure 2C. Examples of CD11c and CD8 costaining (arrows) in the Renca syngeneic tumor. The CD11c antibody is from Cell Signaling Technology, Inc. (product #45581).

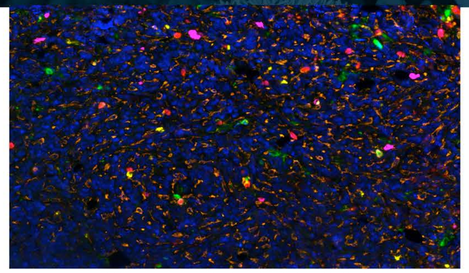

CT26 tumor tissue stained with the described panel (Table 1).

Figure 3A

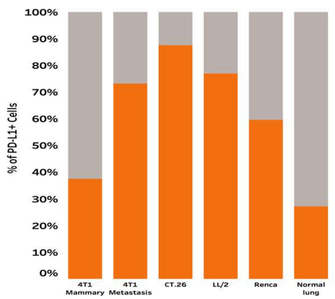

Figure 3B

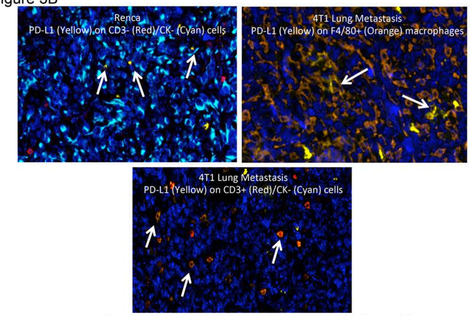

Figure 3A. The percentages of PD-L1+ cells across all 3 fields in each tumor also positive for CD8 (left) or coregistering for F4/80+ (right).
Figure 3B. Representative images of the various patterns of PD-L1 expression patterns observed. From left to right: PD-L1 (yellow) on F4/80+ (orange) cells in the Renca tumor, PD-L1 (yellow) on CK-/F4/80- cells in the 4T1 lung metastasis, and PD-L1 (yellow) on CD3+ (red) cells in the 4T1.ung metastasis.

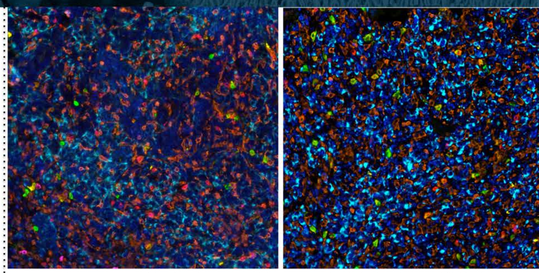

4T1 lung metastasis (L) and 4T1 breast tumor (R) tissue stained with the described panel (Table 1).

Figure 4A

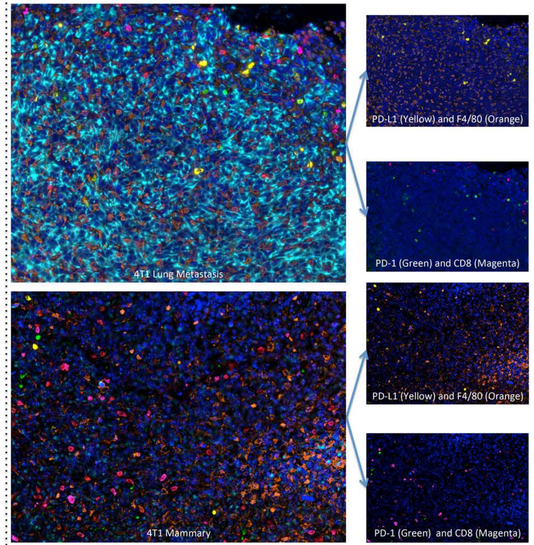

Figure 4A. Images of the 4T1 lung metastasis (top) vs. the 4T1 breast tumor (bottom), with the differences in the frequency of PD-L1/F4/80 comingling as well as that of dual-positive CD8+/PD-1+ cells highlighted in the magnified boxes below each image.

Cell Signaling TECHNOLOGY®

For Research Use Only. Not For Use in Diagnostic Procedures

Presenter Name
email: presenter@cellsignal.com
www.cellsignal.com/posters